Materials Today: Proceedings 63 (2022) S385–S390

Contents lists available at ScienceDirect

Materials Today: Proceedings

journal homepage: www.elsevier.com/locate/matpr

Variation of annealing temperature with excess of NaOH concentration on Ag_2S synthesis from argentometry titration waste as NTC thermistor

Gunawan *, Deborah Sinaga, Muhammad Cholid Djunaidi, Abdul Haris

Chemistry Department, Diponegoro, University, Semarang 50271, Indonesia

ARTICLE INFO

Article history:
Available online 8 April 2022

Keywords:
Silver sulfide
Annealing
NTC

ABSTRACT

Utilization of AgCl from argentometric titration waste can be done by converting AgCl into silver sulfide (Ag_2S) semiconductor. The variation of annealing temperature in Ag_2S synthesis affects the properties and quality of the Ag_2S semiconductor. Silver sulfide semiconductor can be applied as a NTC (negative temperature-coefficient) thermistor temperature sensor. The NTC thermistor shows a decrease in resistance with increasing temperature. This study aims to synthesize Ag_2S from argentometric titration waste with excess NaOH concentration and variations in annealing temperature as a temperature sensor for NTC thermistors. Ag_2S was synthesized using thiourea reagent in alkaline NaOH medium. The synthesized silver sulfide was then annealed at various temperatures of 100, 200 and 300 °C for 30 min. Ag_2S was then characterized using Thermo Gravimetrical Analysis (TGA), X-Ray Diffraction (XRD) and UV–Vis Diffuse Reflectance Spectroscopy (UV–Vis DRS). The results of TGA analysis showed that Ag_2S at a temperature of 836 °C had decomposed into Ag and S_2. From the XRD characterization results showed the presence of Ag_2S at 2θ peaks of 22; 29; 31; 38 and 41°. Ag_2S crystal size increases with increasing annealing temperature, which are 37.04; 39.55 and 41.68 nm. The results of UV–Vis DRS characterization showed that the Ag_2S band gap value decreased with increasing annealing temperature, which were 0.96; 0.94; and 0.92 eV. The resistance measurement results show that the Ag_2S semiconductor at annealing temperature of 300 °C is an NTC thermistor with good electrical quality, has a sensitivity of 6.85% and a thermistor constant of 6087 K.

1. Introduction

Silver compounds in research in the laboratory and the organic industry are very important. One of them is the use of $AgNO_3$ as a source of silver for argentometric titration with the Fajans, Mohr and Volhard methods to analyze the analyte content accurately. However, the argentometric titration process produces large amounts of AgCl precipitate residue [1]. AgCl waste residue, if directly disposed of, will be harmful to the environment. So it is necessary to reuse AgCl waste into something useful. One of them is by reusing AgCl waste by recycling it into silver sulfide (Ag_2S) which is more environmentally friendly.

Silver sulfide is the most widely used sulfide semiconductor besides lead, zinc, cadmium and copper(I) sulfides. The Ag_2S semiconductor has three modified polymorphs (α-Ag_2S, β-Ag_2S dan γ-Ag_2S) at close temperature intervals, this causes Ag_2S to have different structures and properties. The transition between semiconductor α-Ag_2S and superionic β-Ag_2S has unique characteristics [2]. Ag_2S semiconductor has a bandgap of 0.9–1.05 eV [3], chemical stability and good optical properties, so it is widely used in various fields [4] such as antibacterial agents [5], NH_3 sensors [6] and temperature sensors [2].

The temperature sensor is a heat sensor to detect symptoms of temperature changes in certain dimensions. Symptoms of temperature changes detected can be observed using a thermistor [7]. The thermistor is a passive resistance component that has a high sensitivity to temperature changes. One of the thermistors that are often used is the negative temperature-coefficient (NTC) which has very good sensitivity characteristics and a very fast response

* Corresponding author.
E-mail addresses: gunawan@live.undip.ac.id (Gunawan), debosinaga156@gmail.com (D. Sinaga), cholidjunaidi@live.undip.ac.id (M.C. Djunaidi), a.haris@live.undip.ac.id (A. Haris).

https://doi.org/10.1016/j.matpr.2022.03.553
2214-7853/

time [8]. Most of the NTC materials are solid solutions of transition metal oxides, such as NiO, Mn_3O_4, and Co_3O_4 with a spinel-type crystal structure of the general formula AB_2O_4, which often exhibit poor stability and reproducibility due to high porosity and incomplete intergranular contact [9]. Therefore, in this study, the use of Ag_2S as an NTC thermistor will be discussed.

Several studies related to Ag_2S synthesis have been successful from Ag^{2+} ions protected under 3-mercaptopropionic acid (Ag/MPA) conditions with annealing temperature of 200℃ [10], from Ag and H_2S sulfurization, from Ag-Ag_2S nanohybrid NHS and its application as antibacterial [11]. However, H_2S has high toxicity, nanohybrids are complicated and expensive. Meanwhile, in this experiment, Ag_2S was produced from artificial AgCl waste in a high concentration NaOH base medium with thiourea and varying annealing temperature. The obtained Ag_2S was then characterized using TGA, XRD, and UV–Vis DRS, as well as an analysis of the effect of annealing temperature on the quality of the Ag_2S semiconductor as an NTC thermistor temperature sensor.

2. Experimental details

2.1. Ag_2S synthesis with excess NaOH concentration

Artificial argentometric titration waste produced by reacting AgCl with $AgNO_3$ was employed in this study. The synthesis of silver sulfide (Ag_2S) began with the preparation of artificial waste silver chloride (AgCl) by dissolving silver nitrate ($AgNO_3$ (Merck)) 20 mmol in 10 mL of distilled water and dissolving sodium chloride (NaCl (Merck)) 20 mmol in 10 mL of distilled water in a different beaker. Then a solution of silver nitrate ($AgNO_3$) was mixed with a solution of sodium chloride to form a white precipitate of silver chloride (AgCl). Furthermore, the filtered silver chloride (AgCl) precipitate was dissolved in 100 mL of 0.1 M NaOH (Merck) and heated with a hotplate stirrer until it reached a temperature of 60 ℃. When the temperature of the solution reached 60℃, thiourea (Merck) powder 10 mmol was added and a black precipitate of Ag_2S was formed. The black precipitate obtained was filtered and dried in an oven at 60℃ for 60 min. Then the Ag_2S powder was annealed using a furnace with various annealing temperatures of 100, 200, and 300 °C.

2.2. Ag_2S characterization

The synthesis results were analysed using Thermo Gravimetrical Analysis (TGA) Exstar SII 7300 to determine the mass loss due to the synthesis temperature. Ag_2S with varied annealing temperature was characterized using X-Ray Diffraction (XRD) Shimadzu XRD-7000 to determine the crystallinity and the presence of Ag_2S compounds in the precipitate. Characterization with UV–Vis Diffuse Reflectance Spectroscopy (UV–Vis DRS) Shimadzu UV-2430 was used to analyse the band gap of Ag_2S.

2.3. Preparation of thermistor temperature sensor

The annealed Ag_2S powder was put in a press tool and pressed using a hammer with added copper wire on each side of the pellet. Then the pellet was coated with black paint so that the thermistor was not brittle.

2.4. Ag_2S thermistor resistance measurement

Resistance measurement used multimeter (Krisbow). The thermistor was immersed in a container filled with oil and heated on a hot plate with a temperature range of 25-50℃. Resistance was measured every 1℃-temperature increase.

3. Results and discussions

3.1. Ag_2S synthesis

Ag_2S synthesis was carried out by reacting AgCl and thiourea as a silver and sulfur sources, respectively. The synthesis was carried out by reacting AgCl and NaOH excess. Excess of NaOH will accelerate the formation of Ag_2S nanoparticles [12]. The formation of Ag_2S at low pH (<10) occurs slowly [13]. The ratio of moles of reactants is presented in the following equation (1):

	$AgCl_{(s)}$ +	$NaOH_{(aq)}$ →	$AgOH_{(s)}$ +	$NaCl_{(aq)}$
Initial	: 0.02	0.06	-	-
Reaction	: 0.02	0.02	0.02	0.02
Final	: -	0.04	0.02	0.02

(1)

The NaOH reactant does not completely react so that there is an excess of NaOH at equilibrium. NaOH causes silver ions and sulfur ions to hydrolyze in solution to form Ag_2S. AgCl (K_{sp} AgCl 1.6×10^{-10}) will be hydrolyzed by NaOH and make the solution very alkaline, so a blackish brown precipitate of AgOH is formed. The mixed solution was then stirred at 60℃ in a water bath. Thiourea was added while heated and stirred to speed up the reaction. Thiourea or $(NH_2)_2CS$ is an organosulfur which is used as a source of sulfur in the synthesis of metal sulfides [14].

Thiourea will be hydrolyzed by OH^- thus weakening the C = S bond. The mechanism for the release of S^{2-} in thiourea and the formation of silver sulfide in the following equation (2–4) [14]:

$$Ag^+ + (NH_2)_2CS + OH^- \rightarrow HS^- + H_2NCN + Ag^+ + H_2O \quad (2)$$

$$Ag^+ + HS^- + OH^- \rightarrow Ag^+ + S^{2-} + H_2O \quad (3)$$

Overall reactions:

$2Ag^+ + 2OH^- + (NH_2)_2CS \rightarrow 2Ag^+ + S^{2-} + H_2NCN + 2H_2O$.

$$2AgOH_{(s)} + (NH_2)_2CS_{(aq)} \rightarrow Ag_2S_{(s)} + H_2NCN_{(aq)} + 2H_2O_{(aq)} \quad (4)$$

The synthesized Ag_2S was then annealed in a furnace with temperature variations of 100, 200 and 300℃. The annealing process was carried out to recrystallize the silver sulfide.

3.2. Ag_2S characterization

3.2.1. Characterization with TGA

Ag_2S samples were measured at a temperature of 27 to 1000℃ with a heating rate of 10℃/min using TGA to determine the amount of Ag_2S mass lost when heat treated. The results of the TGA Ag_2S analysis in Fig. 1 show that the sample weight decreases with increasing temperature. The TGA curve shows that there are two stages of mass loss. The first mass loss at 253 is 12.19% which is indicated due to the evaporation of water and impurities in Ag_2S crystals. These results are following the literature [15]. Then the second step up to a temperature of 836℃ Ag_2S loses mass of 15.59% as the process of decomposition of Ag_2S into sulfur as the following reaction equation (5) [16].

$$Ag_2S\ (s) \rightarrow 2Ag\ (s) + S_2\ (g) \quad (5)$$

Fig. 1 shows that at a temperature of more than 300℃ there is a decrease in the weight or decomposition of Ag_2S. Therefore, the Ag_2S annealing process is limited to that temperature (annealing temperature is set at 100, 200 and 300℃).

3.2.2. Characterization with XRD

X-ray characterization was carried out with Cu Kα1 (1.5406) radiation at an angle range of 2θ from 20 to 70°. The results of the Ag_2S X-ray diffraction analysis used the RRUFF standard num-

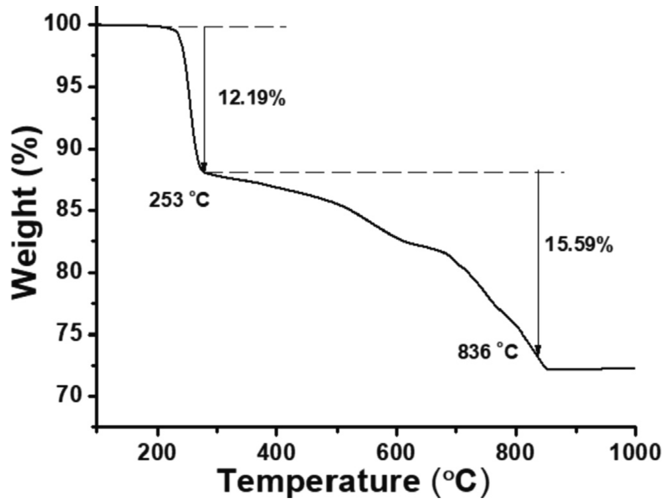

Fig. 1. TGA curve of Ag_2S.

ber R080016 as a comparison. Fig. 2 shows the results of the Ag_2S X-Ray Diffraction analysis with variations in annealing temperature of 100, 200 and 300℃. The diffraction pattern of each temperature variation gives a 2θ peak that is similar and dominant at 22.36° (crystallographic plane (111), 26.189° (111), 29.05° (012), 31.62° (120), 33.66° (121), 34.74° (112), 36.80° (022), 37.79° (200), 40.85° (031), 43.47° (130), 46.28° (202) and 53.21° (004). Another research group on silver sulfide [17,18], has observed a similar crystal structure with diffraction peaks suitable for different synthesis techniques. Ben Nasrallah et al. [19] reported on a Silver sulfide thin film annealed in a nitrogen atmosphere crystallized in the β-Ag_2S phase with orientation (103), Barrera-Calva et al. [20] reported on an Ag_2S thin film crystallized in the α-Ag_2S (acanthite) phase, shows the low-intensity diffraction peaks that occur at Bragg angles of 34.48°, 36.56° and 44.28° correspond to (100), (112), and (121). This study could be determined according to the data reported for α-Ag_2S (acanthite) (JCPDS Card File: 00–014-0072) [21]. This is confirmed by the dominant peak pattern which corresponds to the RRUFF standard for Ag_2S data shown at 2θ peak 22; 29; 31; 38 and 41° [22] and indexed in the monoclinic. So it can be concluded that Ag_2S has been formed and has been successfully synthesized.

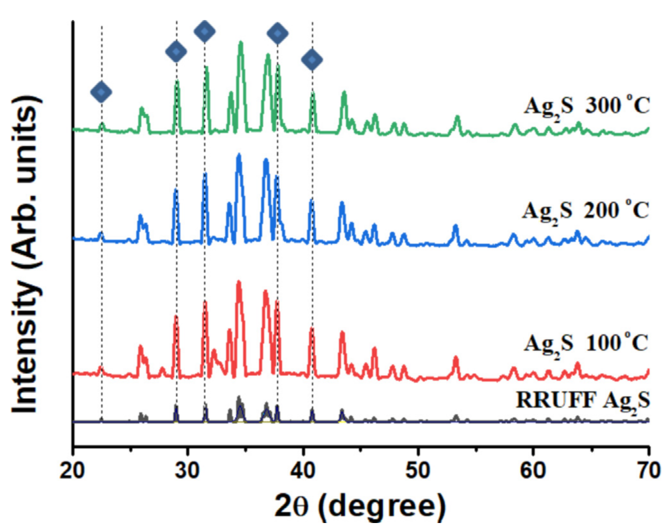

Fig. 2. XRD Diffractogram of Ag_2S at RRUFF, 25℃, annealed at 100, 200 and 300℃, respectively.

The effect of increasing the annealing temperature is directly proportional to the increase in the intensity of Ag_2S crystallinity. The higher the increase in temperature, the more the crystallinity of silver sulfide [23]. This is because more and more impurities are evaporated, so the crystalline material is purer and has higher intensity.

Determination of the grain size of Ag_2S crystals was estimated using the Debye-Scherrer equation [24]:

$D = \frac{k\lambda}{\beta \cos\theta}$where, D is the crystal size, k is the Scherrer constant (0.94), λ is the wavelength of X-ray radiation (0.15406 nm), β is the FWHM in radians and θ is the Bragg angle. From the results of the calculations in Table 1, it is known that the smaller the FWHM, the larger the crystal grain size and the smaller the diffraction pattern, on the contrary, the larger the FWHM value, the smaller the crystal size and the larger the diffraction pattern.

The average grain size of Ag_2S crystals with variations in annealing temperature of 100, 200 and 300℃ was obtained at 37.04; 39.55 and 41.68 nm. This shows that the increase in annealing temperature causes a change in the crystal grain size and Ag_2S crystallization. The higher the annealing temperature, the larger the crystal size obtained, according to the literature [25]. The annealing process causes the growth of a more regular crystal structure which increases the size of the crystal grains. This could be due to a fragmentation of the crystallites at the higher annealing temperatures and/or a re-evaporation of sulphur during the annealing process [26].

3.2.3. Characterization with UV–Vis DRS

The characterization was carried out at a wavelength from 200 to 800 nm based on the intensity measurement of the UV–Vis light reflected by the Ag_2S sample. The determination of the band gap value is obtained from the Tauc Plot calculation by extrapolating from the graph of the relationship E_g = hυ as the abscissa and $(\alpha h\upsilon)^2$ as the ordinate until it intersects the energy axis [25]. The band gap energies obtained (Fig. 3) at annealing temperature variations of 100, 200 and 300℃ are 0.96, 0.94 and 0.92 eV, respectively. This shows that increasing the annealing temperature will decrease the bandgap value.

Ag_2S annealing at a temperature of 100℃ has the largest bandgap energy which will result in low-efficiency performance because wide energy will require a large amount of energy to jump electrons from the valence band to the conduction band to generate current. On the other hand, narrow bandgap energy at an annealing temperature of 300℃ will allow the semiconductor to

Table 1
The crystal size of synthesized Ag_2S with variations of annealing.

Semiconductor	2θ	FWHM	D (nm)
Ag_2S (*Annealing* at 100 °C)	22.36	0.236	35.81
	28.96	0.236	36.28
	31.49	0.197	43.81
	37.72	0.276	31.83
	40.73	0.236	37.47
			Average = 37.04
Ag_2S (*Annealing* at 200 °C)	22.46	0.236	35.82
	28.94	0.197	43.55
	31.47	0.197	43.81
	37.69	0.236	37.12
	40.74	0.236	37.47
			Average = 39.55
Ag_2S (*Annealing* at 300 °C)	22.53	0.197	42.99
	29.05	0.197	43.56
	31.62	0.197	43.82
	37.79	0.236	37.13
	40.85	0.217	40.9
			Average = 41.68

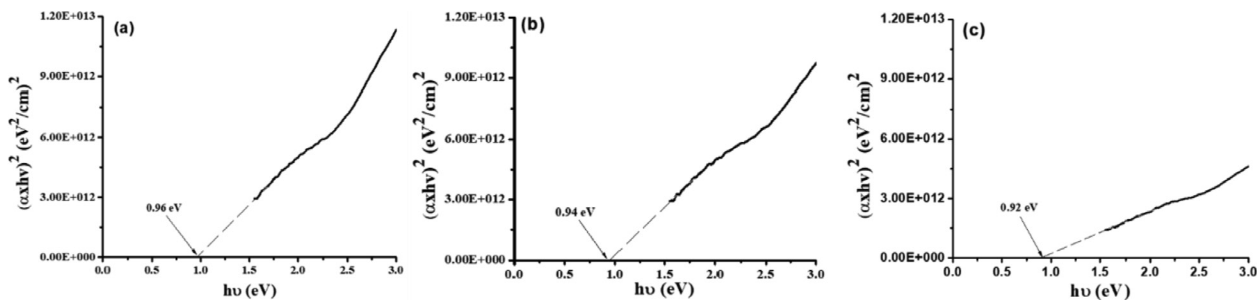

Fig. 3. Band gap of Ag_2S synthesis at annealing temperature of (a) 100℃ (b) 200℃ (c) 300℃.

produce the best electrical current that is correlated with its resistivity and is suitable for the needs of the thermistor.

The bandgap value obtained is 0.9–1.05 eV, following previous studies [3,4,26]. So that the Ag_2S obtained is a suitable semiconductor for the use of thermistors because in the bandgap the semiconductor can absorb infrared wavelengths (1290.62 – 1346.74 nm) which produces heat.

3.3. Preparation of Ag_2S thermistor pellet

The pellets were made with Ag_2S prepared by annealing variations of 100, 200, and 300℃. Then the annealed Ag_2S was molded and pressed using a hammer (Fig. 4). The resulting pellet is a solid cylindrical shape with a diameter of 0.5 cm and a thickness of 0.1–0.2 cm. Both sides of the pellets were wired and the pellets were coated with black paint to give the pellets rigidity. After the Ag_2S powder was pressed, the Ag_2S thermistor pellets are obtained as shown in Fig. 5.

Fig. 4. Tool for Ag_2S pellet preparation.

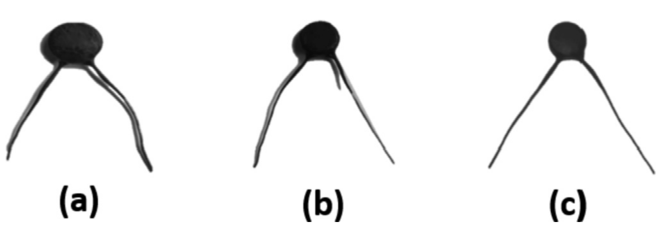

Fig. 5. Ag_2S pellet prepared from Ag_2S powder annealed at (a) 100℃, (b) 200℃ and (c) 300℃.

3.4. NTC Ag_2S thermistor resistance measurement

The resistance measurement of Ag_2S thermistor pellets was aimed to determine the electrical characteristics of the Ag_2S thermistor as an NTC thermistor temperature sensor. Resistance measurement was carried out on changes in temperature using a multimeter. Oil bath temperature for resistance measurement of Ag_2S thermistor was carried out at a temperature variation of 25-50℃.

Based on the graph in Fig. 6, it can be seen that there is a decrease in resistance with increasing temperature. The decrease in resistance that occurs is not linear but exponential. This is in accordance with the theoretical NTC thermistor where the electrical resistance decreases logarithmically as the temperature increases. The inversely proportional relationship between resistance and temperature in the NTC is due to the increasing number of electrons as charge carriers in the conduction band as the temperature increases. The more charge carriers the resistance will decrease [27].

The relationship between resistivity and thermistor temperature is shown in equation (6) [28]:

$$\rho = \rho o \exp\left(\frac{Ea}{kT}\right) \tag{6}$$

Where, ρ = resistivity at temperature T (Ωcm), ρ_o = constant (Ωcm), Ea/k = B = constant of thermistor, and T = temperature (K). The value of constant of thermistor (B) can be obtained by plotting ln ρ vs 1/T as shown in Fig. 7.

Based on Fig. 7 the relationship between ln ρ and 1/T obtained different gradients for each variation of annealing temperature. This gradient value is used to determine the characteristics of the

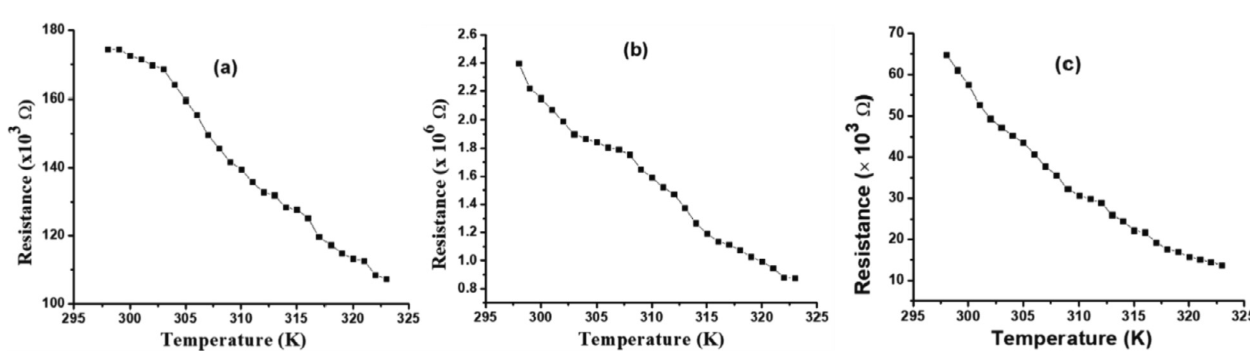

Fig. 6. Correlation graph between resistance of Ag_2S thermistor vs T prepared from Ag2S powder annealed at (a) 100℃, (b) 200℃, and (c) 300℃.

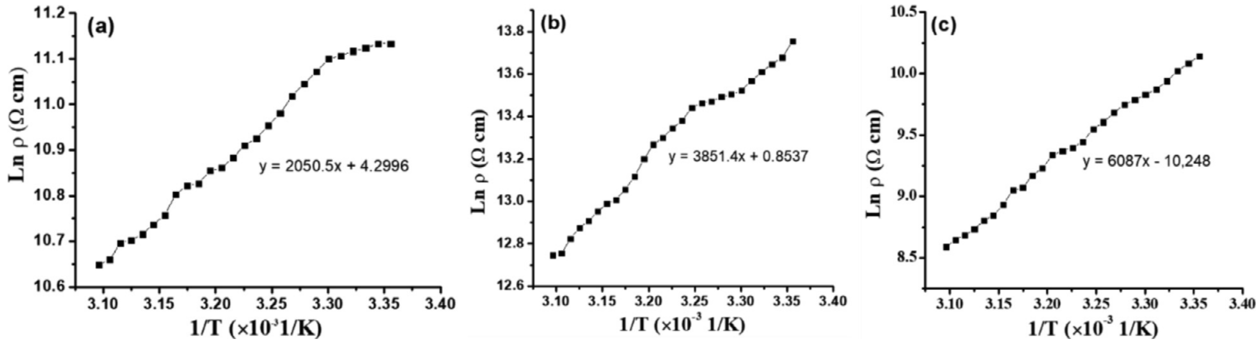

Fig. 7. Correlation graph of ln ρ vs 1/T for sample annealed at (a) 100 °C, (b) 200 °C, and (c) 300 °C.

Table 2
NTC thermistor constants and sensitivity.

Annealing (°C)	B (K)	α (%)
100	2050	−2,30
200	3851	−4,33
300	6087	−6,85

Ag_2S thermistor, namely the thermistor constant value (B). From this constant value, the thermistor sensitivity (α) can be determined by using equation (7) [27]:

$$\alpha = -\frac{B}{T^2} \text{x}\, 100\% \tag{7}$$

Where, α = sensitivities thermistor, B = constant of thermistor, and T = temperature (K).

The results of the calculation of the quality characteristics of the NTC thermistor from the synthesized Ag_2S are presented in Table 2, namely by obtaining the thermistor constant and sensitivity data. Based on Table 2 the characteristics of the synthesized thermistor with annealing temperature of 300 °C is the thermistor with the best response to temperature changes because it has the best sensitivity. The annealing temperature increases the thermistor constant value [24,29,30]. The increase in the thermistor constant is due to the relationship of crystal growth with higher annealing temperatures, resulting in larger crystal grains. The thermistor constants and sensitivity produced on the NTC Ag_2S thermistor at annealing temperature of 300 °C are 6087 K and 6.85%, respectively. This value is in accordance with the research of Taufik et al. [31] where the thermistor constant and sensitivity of the synthesized thermistor were 5982 K and 6.73%, respectively.

4. Conclusion

The synthesis of Ag_2S with excess NaOH at various annealing temperatures causes an effect on the crystal grain size, bandgap and quality of the Ag_2S NTC thermistor. The NTC Ag_2S thermistor with annealing temperature of 300 °C is very sensitive to temperature changes. The thermistor constant and the resulting sensitivity are 6087 K and 6.85%.

CRediT authorship contribution statement

Gunawan: Conceptualization, Methodology, Project administration, Resources, Validation, Writing – review & editing. **D. Sinaga:** Data curation, Formal analysis, Investigation, Methodology, Validation, Writing – original draft, Writing – review & editing. **M.C. Djunaidi:** Data curation, Formal analysis, Investigation, Methodology, Validation, Writing – original draft, Writing – review & editing. **A. Haris:** Data curation, Formal analysis, Investigation, Methodology, Validation, Writing – original draft, Writing – review & editing.

Declaration of Competing Interest

The authors declare that they have no known competing financial interests or personal relationships that could have appeared to influence the work reported in this paper.

Acknowledgements

The authors are thankful to selain-APBN FSM UNDIP 2021 for funding this work.

References

[1] A.G. Mtewa, D.C. Sesaazi, S.K. Botchie, E.L. Peter, S. Deyno, B.A. Neme, D. Mweta, Academic Press (2022) 103–113.
[2] S.I. Sadovnikov, A.I. Gusev, J. Mater. Chem. A Mate. Energy Sustain. 5 (34) (2017) 17676–17704.
[3] S.I. Sadovnikov, A.I. Gusev, Biointerface Res. Appl. Chem. 6 (6) (2016) 1797–1804.
[4] C. Cui, X. Li, J. Liu, Y. Hou, Y. Zhao, G. Zhong, Nanoscale Res. Lett. 10 (1) (2015) 1–21.
[5] Y.D. Beleno, C.E.M. Nunez, M.C. Valadez, N.S.F. Lopez, M.F. Acosta, Mater. Res. Bull. 99 (2018) 385–392.
[6] T. Fu, Electrochim. Acta 121 (2014) 168–174.
[7] M.B.U. Kaleka,. OPTIKA: Jurnal Pendidikan Fisika 1 1 (2017) 8–11.
[8] G. Lei, H. Chen, S. Zheng, F. Lou, L. Chen, L. Zeng, J. Zhang, Q. Zhao, C. Yang, J. Material Sci. Material Electron 24 (2013) 1203–1207.
[9] R. Schmidt, A. Basu, A.W. Brinkman, J. Eur. Ceram. Soc. 24 (2004) 12331236.
[10] M. Yu, D. Liu, W. Li, X. Zhou, Appl. Surf. Sci. 288 (2014) 158–165.
[11] S.K. Gahlaut, P. Devi, J.P. Singh, Appl. Surf. Sci. 528 (2020), 147037.
[12] W.D.P. Rengga, A. Yufitasari, W. Adi, Jurnal Bahan Alam Terbarukan 6 (1) (2017) 32–38.
[13] I. Grozdanov, Appl. Surf. Sci. 84 (3) (1995) 325–329.
[14] J.A. García-Valenzuela, Comments Inorg. Chem. 37 (2) (2017) 99–115.
[15] D. Qin, L. Zhang, X. Du, G. Yang, Q. Zhang, C Indian Academy Of Sciences, Bull. Mater. Sci. 38 (6) (2015) 1665–1671.
[16] V. Piacente, P. Scardala, D. Ferro, J. Mater. Sci. Lett. 9 (3) (1990) 365–367.
[17] J. Li, A. Tang, X. Li, Y. Cao, M. Wang, Y. Ning, L. Lv, Q. Lu, Y. Lu, Y. Hu, Y. Hou, F. Teng, Nanoscale Res. Lett. 9 (2014) 128.
[18] J. Yang, J.Y. Ying, Supplementary Material (ESI) for Chemical Communications, The Royal Society of Chemistry, 2009.
[19] T. Ben Nasrallah, H. Dlala, M. Amlouk, S. Belgacem, J.C. Bernède, Synthetic Materials 151 (2005) 225.
[20] E. Barrera-Calva, M. Ortega-López, A. AvilaGarcía, Y. Matsumoto-Kwabara, ThinSolid Films 518 (2010) 1835.
[21] K.P. Remya, T. Udayabhaskararao, T. Pradeep, J. Phys. Chem. C 116 (2012) 26019–26026.
[22] S.I. Sadovnikov, A.I. Gusev, A.A. Rempel, Adv. Mater. Sci. 41 (2015) 7–19.
[23] H. Metin, M. Ari, S. Erat, S. Durmuş, M. Bozoklu, A. Braun, Mater. Res. 25 (1) (2010) 189–196.
[24] J. Ryu, D.S. Park, R. Schmidt, J Apply Phys. 109 (2011) 11.
[25] K. Sahraoui, N. Benramdane, M. Khadraoui, R. Miloua, C. Mathieu, Sensors & Transducers 27 (Special Issue) (2014) 319–325.
[26] P.E. Agbo, P.A. Nwofe, Int. J. Thin Fil. Sci. Tec. 4 (1) (2015) 9–12.
[27] Y.R. Denny, D. Aribowo, Setrum : Sistem Kendali-Tenaga-elektronika-telekomunikasi-komputer 3 (1) (2016) 8.
[28] M. Zhang, M. Li, H. Zhang, K. Tuokedaerhan, A. Chang, J. Alloy. Compd. 797 (2019) 1295–1298.

[29] J. Ryu, K.Y. Kim, J.K. Choi, B.D. Hanhn, W.H. Yoon, B.K. Lee, D.S. Park, C. Park, J. Am. Ceram. Soc. 92 (12) (2009) 3084–3087.
[30] X. Chen, L. Wang, J. Xu, L. Bian, B. Gao, Mater. Sci. Forum 745–746 (2013) 599–604.
[31] D. Taufik, D. Syarif, S. Karim, Prosiding Seminar nasional Sains dan Teknologi Nuklir PTNBR 17–18 (2007).